Numerical simulation of the flow over a tubercled wing

Mohammed Baghdad[1,*], *Abdelkader* Nehmar[1], and *Ahmed* Ouadha[2]

[1]Institut des Sciences et Technologie, Centre Universitaire El-Wancharissi de Tissemsilt, B.P. 182, 38000 Tissemsilt, Algérie
[2]Laboratoire des Sciences et Ingénierie Maritimes, Faculté de Génie Mécanique, Université des Sciences et de la Technologie Mohamed Boudiaf d'Oran, Oran El-M'nouar, 31000 Oran, Algérie

Abstract. The objective of the present study is to carry out a numerical study of the flow around a NACA0021 modified wing by the incorporation of sinusoidal tubercles on its leading edge at a Reynolds number equal to 225,000. The *SST k-ω* turbulence model is used as closure to the incompressible governing equations. Runs have been performed for several attack angles. Results show that for lower angles of attack, tubercles reduce the drag coefficient with a slight increase in lift.

1 Introduction

Fauna and flora have always inspired humankind in their inventions and problem solving. Several technologies in all fields of science have been developed by the observation of nature. This approach, known also as biomimetic, has been widely adopted in the design of submarines and marine propellers in order to reduce drag. In particular, the performance of airfoils can be improved by generating streamwise vortices in boundary layer using tubercled leading edge inspired by prior studies carried out by marine biologists on the morphology of humpback whales pectoral flippers [1-2]. They demonstrated that the high aspect ratio with large sinusoidal tubercles along the flipper leading edge can cause a considerable increase in the stall angle of attack and the maximum lift coefficient.

Several studies have been performed on tubercled leading edge wings during the last years. In particular, experimental studies have demonstrated their benefits. Generally, in most studies, the utilization of airfoils with tubercled leading edge showed improved performance in terms of lower drag, higher lift and shorter separation region. However, in some studies, it is found an opposite trend. Experimental studies aimed to measure lift, drag and pitching moments for various attack angles in wind tunnels. Results are generally analyzed by varying amplitude and wavelength of tubercles. Table 1 summarizes previous experimental studies on tubercled wings.

Recent applications of CFD to solve the Navier-Stokes equations for tubercled wings are summarized in Table 2. In most of studies, in-house research codes that are rarely available for researchers have been used. It is more convenient to perform studies in this topic using available commercial CFD codes such as Fluent. The latter can solve laminar and turbulent, incompressible and compressible, 2D and 3D, steady and unsteady flows.

The conflicting findings observed in the literature regarding the effect of tubercles on the performance of wings make this topic a challenging subject. Further studies are necessary and the present paper constitutes one.

2 Mathematical model

Two NACA 0021 wings designed, built and tested by Bolzon et al. [21] have been used in the present study. One wing had a smooth leading edge, whereas the other wing had tubercles with amplitude of 10.5 mm and a wavelength of 60 mm along its entire leading edge as depicted in Figure 1. Both wings had a span of 330 mm, a Mean Aerodynamic Chord of 130 mm and a taper ratio of 0.4.

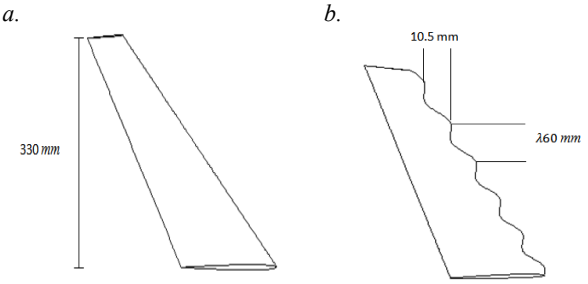

Fig. 1. Geometry of wings studied : *a.* Conventional wing ; *b.* Tubercled wing

The three-dimensional, incompressible and steady Reynolds averaged Navier–Stokes equations are given below:

$$\frac{\partial \overline{u}_i}{\partial x_i} = 0 \tag{1}$$

$$\frac{\partial \left(\overline{u}_i \overline{u}_j\right)}{\partial x_j} = -\frac{1}{\rho}\frac{\partial \overline{p}}{\partial x_i} + \nu \frac{\partial^2 \overline{u}_i}{\partial x_j^2} + \frac{1}{\rho}\frac{\partial \overline{R}_{ij}}{\partial x_j} + \overline{g}_i \tag{2}$$

* Corresponding author: baghdad.cut@gmail.com

Table 1. Previous experimental studies on tubercled wings

Reference	Profile	*A/c*	*λ/C*	*Re*	*α*
Miklosovic et al. [4]	NACA 0020	/	/	5.05×10^5– 5.20×10^5	-2÷20°
Miklosovic and al. [5]	NACA 0020	0.04	/	274,000–277,000	-2÷20°
Johari and al. [6]	NACA 634-021	0.025, 0.05, 0.12	0.25, 0.5	1.83×10^5	-6÷30°
Hansen and al. [7]	NACA 0021	0.03÷0.11	0.11÷0.43	1.2×10^5	0÷20°
Hansen and al. [8]	NACA 0021 NACA65-021	0.028÷0.114	0.1÷0.43	1.2×10^5	0÷25°
Guerreiro and Souse [9]	NASA LS(1)-0417	0.06, 0.12	0.25, 0.5	1.4×10^5 0.7×10^5	0÷30°
Hansen and al. 10]	NACA 0021	0.03÷0.11	0.11÷0.43	1.2×10^5	1÷8°
Chen and al. [11]	FLAT-PLATE E=3 MM	2.5, 5, 12	0.16, 0.21, 0.31	2.7×10^5	/
Sudhakar and Karthikeyan [12]	NACA 4415	0.1	0.25	1.2×10^5	6°
Zverkov and al. [13]	Z 15-25	0.01	0.12	1.2×10^5 1.4×10^5	-20÷20°
Bolzon and al. [14]	NACA 0021	0.0233	0.174	2.2×10^5	-2÷10°
Keerthi and al. [15]	NACA65209	0.033, 0.067	0.083, 0.0125	/	-5, -3,1, 5, 9,13, 17°
Custodio and al. [16]	$NACA63_4$-021	0.025, 0.05, 0.12	0.25, 0.5	9×10^4÷4.5×10^5	0÷30°
Wei and al. [17]	$NACA63_4$-021	0.025, 0.05, 0.12	0.25, 0.5	1.4×10^4	0, 10, 15, 20°
Wei and al. [18]	SD7032	0.12	0.5	1.4×10^4	15°
Bolzon and al. [19-20-21]	NACA 0021	A=10.5	Λ=60	2.25×10^5	/
Keerthi and al. [22]	NACA 65209	0.033, 0.066	0.125, 0.166	1.3×10^5	-5÷20°
Wei and al. [23]	$NACA63_4$-021	0.12	0.25	/	0, 10, 15, 20°
Qiao and Tong [24]	NACA 0012	0.025, 0.05, 0.1	0.1, 0.2, 0.4	$2\div8\times10^5$	0, 5, 10, 15°
Peristy and al. [25]	NACA 0018	0.03, 0.04, 0.05, 0.06	0.11, 0.13, 0.18, 0.21	7.5×10^4, 1.5×10^5, 3×10^5	0÷30°

The Reynolds stress tensor $\overline{R}_{ij}$ is approximated using one of the different turbulence models provided in the CFD commercial software Fluent. A careful analysis of the literature reveals that there is no agreement on the selection of turbulence models in the analysis of the flow around tubercled wings. However, it seems that SST k-ω provides better performance in predicting the flow structure around a tubercled wing.

The computational domain has been created according to experiments by Bolzon et al. [21] in a wind tunnel. The domain has an inlet section of 0.5×0.5 m and a length of 2.2 m. The wing is placed at a distance of 0.45 m from the inlet.

The domain has been meshed using a multi block technique. A block represented by a cylinder containing the wing to allow its rotation in order to obtain the desired angle of attack and a second block for the remaining domain. Figure 2 depicts an overview the computational domain.

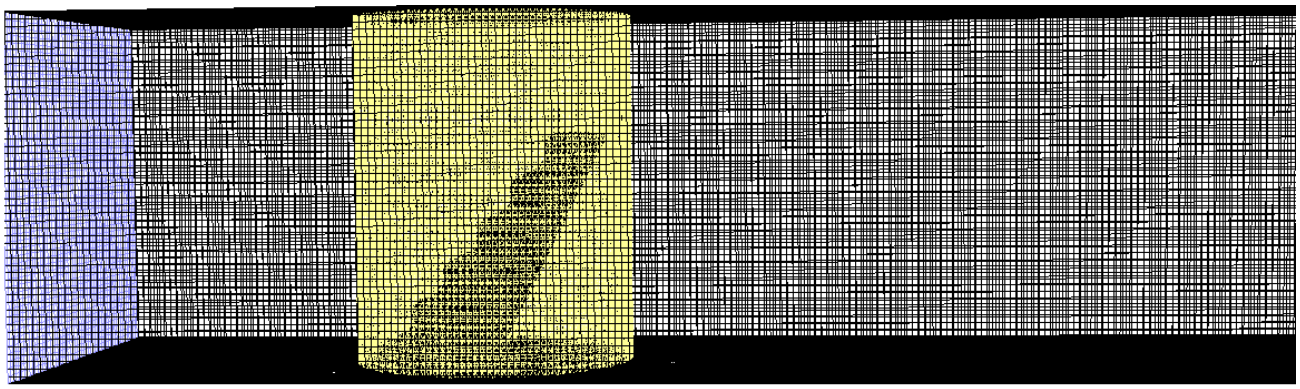

Fig. 2. Computational domain meshing

* Corresponding author: baghdad.cut@gmail.com

The steady Reynolds averaged Navier-Stokes equations, the turbulence model equations and the corresponding boundary conditions have been numerically solved using the pressure based solver of the commercial *CFD* code Fluent. A second order upwind scheme has been selected to discretize momentum and turbulence terms. The algorithm *PRESTO* is used to compute the coupling between the pressure and the velocity field. The runs were assumed to reach convergence once the residuals fall below the value of 10^{-6} for all variables.

Table 2. Previous numerical studies on tubercled wings

Reference	Profile	*A/c*	*λ/C*	*Re*	*α*	Turb.	Code
Favier and al. [26]	NACA0020	0÷0.1	0.25÷2	800	20	/	In-house
Swanson and Isaak [27]	NACA 63_4-021 NACA0020	0, 2.5, 5, 10%	0, 4 ET 8	1.8×10^5 6.3×10^5	0°, 4°, 8°,12°	/	Fluent
Zhang and Wu [28]	S809	0.0125-0.0375	0.17-0.42	Wind speed 7-10-15-20-25 M/S	/	*S-A*	Fluent
Feng and al. [29]	NACA0020	0.0442	1.32	1.35×10^5	0÷26°	*k-ε RNG*	In-house
Kim and al. [30]	NACA0020	0.05	0.75, 0.375, 0.25, 0.1875	10^6	0÷40°	*k-ε Realizable*	Fluent
Lohry and al. [31]	NACA0020	0.05	0.4	5×10^5	0÷20°	*S-A SST*	In-house
Abdel Gawad [32]	NACA0012	0.05	0.2	10^6	0÷20°	*k-ε*	In-house
Câmara and al. [33]	NASA LS(1)-0417	0.12	0.5	1.6×10^5	0÷20°	*k-ω SST*	In-house
Corsini and al. [34]	NACA0015 NACA4415	0.025	0.25	1.83×10^5	0÷30°	*k-ε*	In-house
Lau and al. [35]	NACA0015			3.6×10^5	-1÷4°		In-house
Skillen and al. [36]	NACA0021	0.015	0.21	1.2×10^5	20°	*LES*	In-house
Xingwei and al. [37]	NACA0014	0.05-0.1	0.25-0.5	10^4	0÷15°	*k-ω SST*	In-house
Aftab and Ahmed [38]	NACA4415	Spherical tubercles	D =0.1-0.2	2.5×10^5	0÷20°	*SA*	Ansys 14.5
Asli and al. [39]	S809	0.025	0.25	10^6	0÷20°	*DES-SST k-ω*	In-house
Cai and al. [40]	NACA634-021	0.025-0.12	0.5	1.83×10^5	0÷30°	*SA*	Fluent
Joy and al. [41]	NACA634-021	0.12	0.25-0.5	1.4×10^4	0÷15°	*k-ω SST*	Fluent
Serson and. Meneghini [42]	NACA0012	0÷0.2	0.25÷1	1000	0÷21°	/	In-house
Cai and al. [43]	NACA 634-021	SINGLE LEADING-EDGE	0.25	10^5	3÷24°	*SA*	Fluent
Kobæk and Hansen [44]	S809	0.015	0.125	10^6	-2÷24°	*k-ω SST*	Star ccm+
Rostamzad and al. [45]	NACA0021	0.028	0.1	0.12×10^6 1.5×10^6	0÷20°	*k-ω SST*	CFX
Zhang and al. [46]	NACA 634-021	0.24	0.25	2×10^5	6,12,18,24,45°	*DES*	In-house
Benaissa and al. [47]	NACA 634-021	0.12	0.5	1.4×10^4	0÷20°	*k-ω SST*	Ansys 17.0.
Pérez-torró and Kim [49]	NACA0021	0.03	0.11	1.2×10^5	20°	*LES*	In-house
Zhao and al. [49]	NACA 634-021	0.12	0.25	2×10^5	0÷60°	*DES*	/In-house

3 Results

The results of the simulations are presented as follows. First, a mesh independency test has been performed in order to ensure that the numerical solution is independent to the size of the grid used. This operation is then followed by a detailed analysis of the flow around the wings in terms of lift coefficient, drag coefficient and streamlines. The results have been plotted at Reynolds number of 0.225 million for angles of attack ranging from 0 to 20°.

3.1 Mesh independency test

A mesh independency test has been performed. Three grids of 1 million, 2 million and 4 million have been used for angles of attack ranging from 0 to 20° at a Reynolds number of 0.225 million. Figure 3 shows a comparison of lift and drag coefficients obtained using

* Corresponding author: baghdad.cut@gmail.com

the three grids. It is observed that similar values are obtained using grids 2 and 3. Thus, results are obtained using a mesh of 2 million cells.

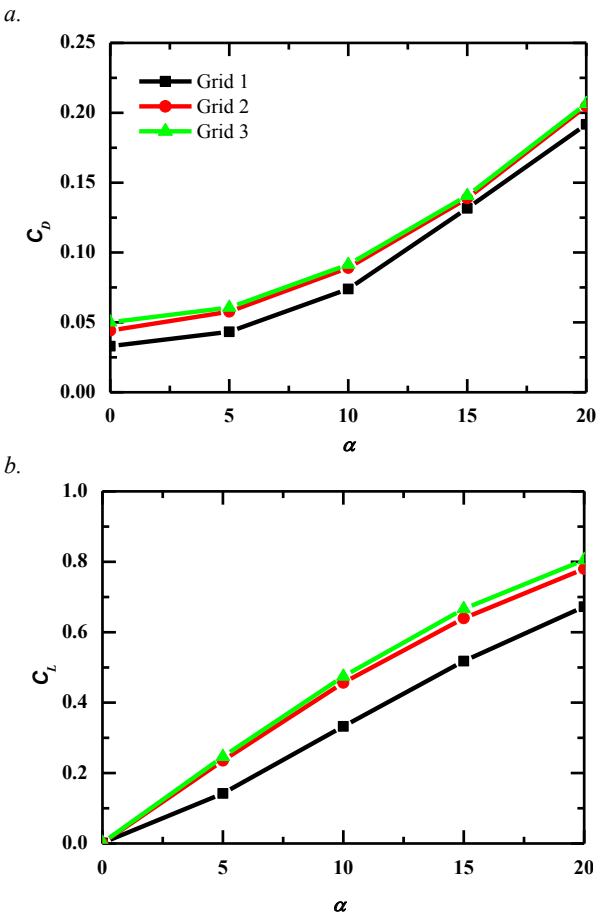

Fig. 3. Mesh independency test: *a*. drag coefficient; *b*. lift coefficient

3.2 Lift and drag coefficients

The effect of the angle of attack on the lift and drag coefficients of wings with smooth and tubercled leading edges is presented in Figure 4. Both lift and drag coefficients increase as the angle of attack increases. For both experimental and numerical data, at lower angles of attack, leading edge tubercles produce lift coefficient slightly greater than smooth leading edge. The difference increases as the angle of attack increases. As stated by many researchers, this trend can be attributed to the formation of a laminar separation bubble on the section side of the wings [10-20, 45]. However, there is no widespread agreement on this finding. The laminar separation bubble on the section side of wings have not been observed by other researchers [4, 6].

For lower angles of attack (α < 8 (for experimental measurement) and α < 12 (for numerical data)), tubercles reduce the drag coefficient as illustrated in Figure 3.*b*. However, for angles of attack greater than these values, tubercles increase the drag coefficient.

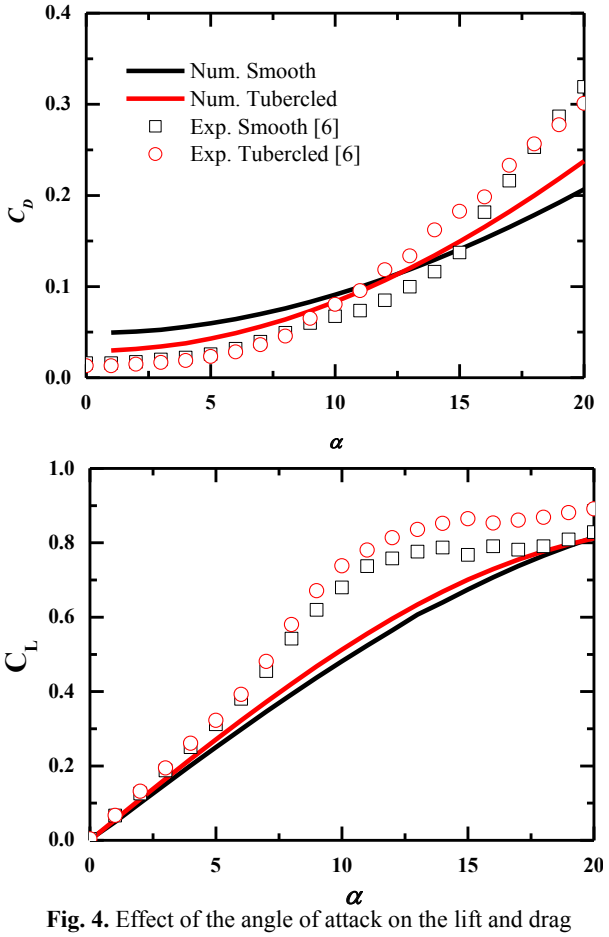

Fig. 4. Effect of the angle of attack on the lift and drag coefficients

3.3 Streamlines

Figure 4 gives a comparison between streamlines colored by the flow velocity obtained for tubercled and smooth wings at angles of attack of 0, 10 and 20°. For α = 0 and 10°, the streamlines behind the wings remain parallel to the free stream. However, the pattern of streamlines at α = 20° is modified with the formation of vortices.

4 Conclusions

The flow around two swept wings, one smooth and one tubercled, has been numerically analyzed using the commercial code Fluent. Turbulence has been modeled using *SST k-ω* model, the most widely used model for this kind of flows. It is found that for lower angles of attack, tubercles reduce the drag coefficient with a slight increase in lift.

The discrepancy between numerical results and experimental measurements at attack angles greater than 5 cannot be attributed to experimental errors as it is observed for both wings. Indeed, under these conditions, laminar separation bubble on the section side of the wings observed in many previous experimental studies appears and SST *k-ω* model falls in predicting correctly the airfoil's pressure distribution.

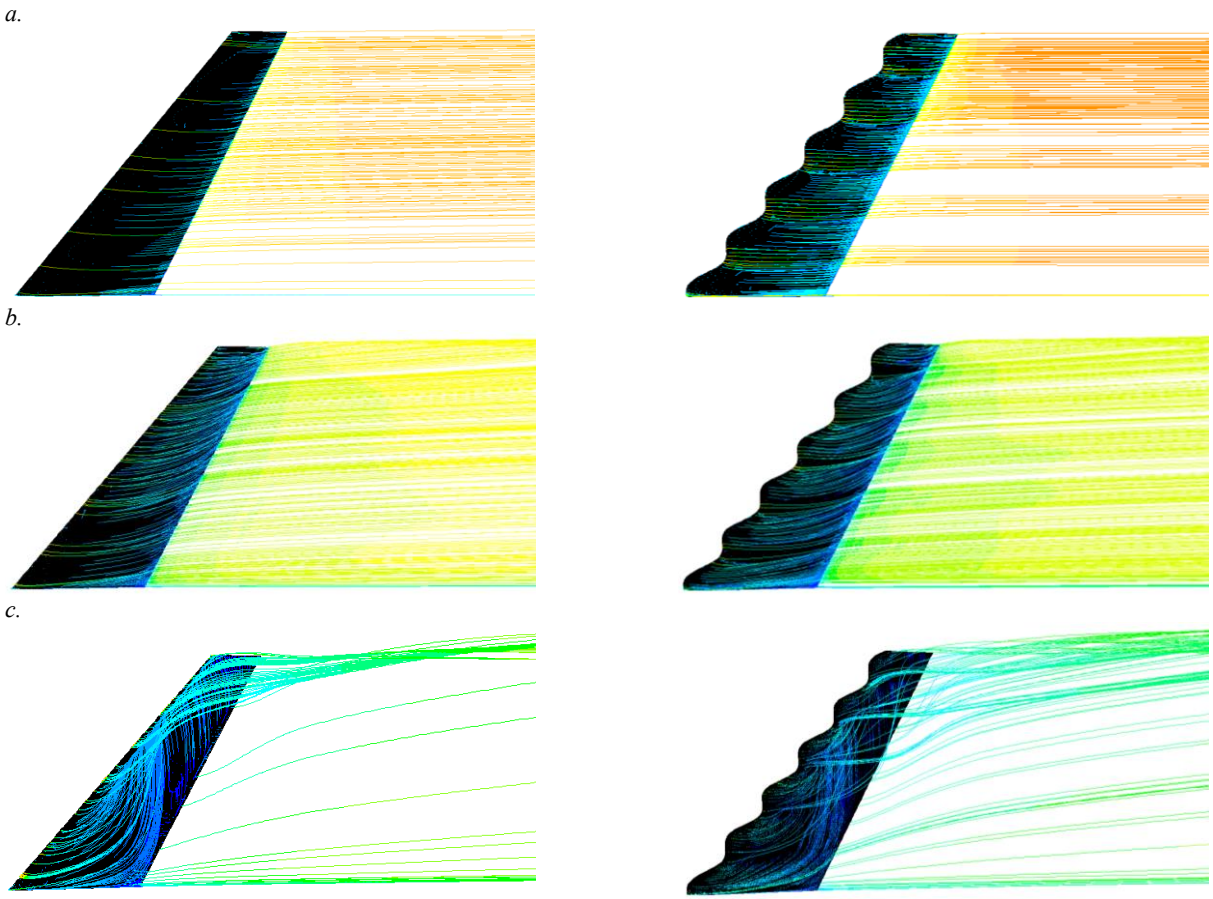

Fig. 5. Streamlines colored by the velocity at an angle of attack angle: *a.* $\alpha = 0°$, *b.* 10°, *c.* 20°

References

1. F.E. Fish, J.M. Battle, J. Morphology, **225 (**1995)
2. F.E. Fish, New Hampshire, 1999
3. K.L. Hansen, Effect of leading edge tubercles on airfoil performance. Ph.D. Dissertation, The School of Mechanical Engineering, The University of Adelaide, South Australia (2012)
4. D. S. Miklosovic, M.M. Murray, L.E. Howle, F.E. Fish, Physics of Fluids, **16 (**2004)
5. D.S. Miklosovic, M.M. Murray, Journal of Aircraft, **44** (2007)
6. H. Johar, C. Henoch, D. Custodio, A. Levshin, AIAA Journal, **45 (**2007)
7. K.L. Hansen, R.M. Kelso, C.J. Doolan, 16th AIAA/CEAS Aeroacoustics Conference (2010)
8. K.L. Hansen, R.M. Kelso, B.B. Dally, AIAA Journal, **49 (**2011)
9. J.L.E. Guerreiro, J.M.M. Sousa, AIAA Journal, **50 (**2012)
10. K. Hansen, R. Kelso, C. Doolan, , Acoustics Australia, **40** (2012)
11. H. Chen, C. Pan, J. Wang, Science china Technological Sciences, **56 (**2013)
12. S. Sudhakar, N. Karthikeyan, The 14th Asian Congress of Fluid Mechanics - 14ACFM October 15 - 19, Hanoi and Halong, Vietnam (2013).
13. I. Zverkov, V. Kozlov, A. Kryukov, Progress in Flight Physics, **5** (2013)
14. M.D. Bolzon, R.M. Kelso, M. Arjomandi, 19th Australasian Fluid Mechanics Conference Melbourne, Australia 8-11 December (2014)
15. M. C. Keerthi, A. Kushari, A. De, A. Kumar, Proceedings of ASME Turbo Expo 2014: Turbine Technical Conference and Exposition, June 16-20, Düsseldorf, Germany (2014)
16. D. Custodio, C.W, Henoch, AIAA Journal, **53**, 7 (2015)
17. Z. Wei, T.H. New, Y.D. Cui, , Ocean Engineering, **108 (**2015)
18. Z. Wei, T.H. New, Y.D. Cui, The 13th International Symposium on Fluid Control, Measurement and Visualization, November15-18, Doha, Qatar (2015)
19. M.D. Bolzon, R.M. Kelso, M. Arjomandi, J. Aerosp. Eng., 04016085 (2016)
20. M.D. Bolzon, R.M. Kelso, M. Arjomandi, EPJ Web of Conferences, **114** (2016)
21. M.D. Bolzon, R.M. Kelso, M. Arjomandi, Aerospace Science and Technology, **56** (2016)
22. M.C. Keerthi, M.S. Rajeshwaran, A. Kushari, A. De, AIAA Journal, (2016)
23. Z. Wei, B. Zang, T.H. New, Y.D. Cui, Ocean Engineering, **121** (2016)
24. W.J. Chen, W.Y. Qiao, F. Tong, , Acte Aeronautica et Astronautica Sinica, **37** (2016)
25. L.H. Peristy, R.E. Perez, A. Asghar, W.D.E. Allan, 34th AIAA Applied Aerodynamics Conference, 13-17 June (2016) Washington, D.C

26. J. Favier, A. Pinelli, U. Piomelli, Preprint submitted to Elsevier Science, 16 septembre (2011)
27. T. Swanson, K.M. Isaac, 6th AIAA Theoretical Fluid Mechanics Conference, 27-30 June (2011) Honolulu, Hawaii.
28. R.K. Zhang, J.Z. Wu, Wind Energ. **15 (**2012)
29. F. Feng, X. Cheng, X. Qi, X. Chang, Applied Mechanics and Materials, **152** (2012)
30. M.J. Kim, H.S. Yoon, J.H. Jung, H.H. Chun, D.W. Park, Int. J Nav Archit Oc Engng, **4 (**2012)
31. M.W. Lohry, D. Clifton, L. Martinelli, Seventh International Conference on Computational Fluid Dynamics (ICCFD7), July 9-13, (2012) Big Island, Hawaii
32. A.F. Abdel Gawad, Transaction on control and mechanical systems, **2**, 5 (2013)
33. J. F. D. Câmara, 51st AIAA Aerospace Sciences Meeting to be held, 7-10 January (2013), Grapevine, Texas, United States of America.
34. A. Corsini, G. Delibra, A.G. Sheard, Journal of Fluids Engineering, **135** (2013)
35. S.H. Lau, S. Haeri, J.W. Kim, Journal of Sound and Vibration, **332 (**2013)
36. A. Skillen, A. Revell, J. Favier, A. Pinelli, U. Piomelli, International symposium on turbulence and shear flow phenomena, August 25-30 (2013) Poitiers, France.
37. Z. Xingwei, S. Graduate, Z. Chaoying, Z. Tao, J. Wenying, Aircraft Engineering and Aerospace Technology: An International Journal, **85** (2013)
38. S.M.A. Aftab, K.A. Ahmad, Applied Mechanics and Materials, **629 (**2014)
39. M. Asli, B.M. Gholamali, A.M. Tousi, Hindawi Publishing Corporation Mathematical Problems in Engineering, **493253 (**2015)
40. C. Cai, Z. Zuo, S. Liu, Y. Wu, Advances in Mechanical Engineering, **7**, 7 (2015)
41. J. Joy, T.H. New, H. Ibrahim, International journal of mechanical aerospace, mechatronic and manufacturing engineering , **10**, 2 (2015)
42. D. Serson, J.R. Meneghini, Procedia IUTAM, **14 (**2015)
43. C. Cai, Z. Zuo, S. Liu, Y. Wu, International Symposium on Transport Phenomena and Dynamics of Rotating Machinery, Hawaii, Honolulu April 10-15 (2016)
44. C.M. Kobæk, M.O.L. Hansen, Journal of Physics: Conference Series, **753 (**2016)
45. N. Rostamzadeh, R.M. Kelso, B. Dally, Theor. Comput. Fluid Dyn., **10 (**2016)
46. M. Zhang, M. Zhao, J. Xu, Proceedings of the ASME 2016 International Mechanical Engineering Congress and Exposition, November 11-17 (2016) Phoenix, Arizona, USA.
47. M. Benaissa, I. Ibrahim, T. New, W. Ho, 2017, Topical problems of fluid mechanics, http://www.it.cas.cz/fm/im/im/proceeding/2017/4
48. R.P. Torró, J.W. Kim, Fluid Mech., **813** (2017)
49. M. Zhao, M. Zhang, J. Xu, Engineering applications of computational fluid mechanics, **11**, 1 (2017)